

# The photophysics of salicylic acid derivatives in aqueous solution

Ivan P. Pozdnyakov<sup>a\*</sup>, Anatolio Pigliucci<sup>b</sup>, Nikolai Tkachenko<sup>c</sup>,  
Victor F. Plyusnin<sup>a</sup>, Eric Vauthey<sup>b</sup> and Helge Lemmetyinen<sup>c</sup>

The photophysics of a number salicylic acid derivatives (SADs) in aqueous solutions was investigated in a wide range of pH by time-correlated single photon counting ( $\lambda_{\text{ex}} = 350 \text{ nm}$ ,  $\tau_{\text{resp}} = 300 \text{ ps}$ ) and fluorescence up-conversion ( $\lambda_{\text{ex}} = 266 \text{ nm}$ ,  $\tau_{\text{resp}} = 300 \text{ fs}$ ) techniques. The acid–base equilibrium constants in the ground ( $\text{p}K_{\text{a}}$ ) and the excited states ( $\text{p}K_{\text{a}}^*$ ), the fluorescence quantum yields as well as the lifetimes of anionic, neutral, and cationic forms of SADs were determined. Evidence of ultrafast excited-state intramolecular proton transfer (ESIPT) leading to the formation of the proton-transferred excited state of SADs was obtained from the fluorescence up-conversion measurement. The nature of the ESIPT process is discussed. Copyright © 2008 John Wiley & Sons, Ltd.

**Keywords:** Salicylic acid derivatives; fluorescence; ESIPT; up-conversion technique

## INTRODUCTION

Salicylic acid (2-hydroxybenzoic acid) (SA) and its derivatives (SADs) are the simplest systems for studying excited-state intramolecular proton transfer (ESIPT).<sup>[1–13]</sup> On the other hand, SADs are considered as representatives of the complexing functional groups in humic substances and can serve as model compounds for investigating the photochemical properties of natural humic and fulvic acids.<sup>[14]</sup>

The fluorescence properties of SA and SADs have been studied in the gas phase and in series of polar (water, ethanol, dimethylformamide, chloroform) and nonpolar solvents (benzene, *n*-heptane, isooctane, methylcyclohexane).<sup>[1–13]</sup> In the gas phase and in nonpolar solvents, the ground state of SA and SADs exists in two rotameric forms, A and B (Fig. 1a). Rotamer A is thermodynamically more stable than B (enthalpy difference of 14 and 10  $\text{kJ} \cdot \text{mol}^{-1}$  for SA and methyl salicylate (MS)<sup>[5,15]</sup>) due to a strong intramolecular hydrogen bond between the carboxyl and hydroxyl groups.

Rotamer A is characterised by a large Stokes shift of the fluorescence ( $\lambda_{\text{em}} \approx 440 \text{ nm}$ ), while rotamer B exhibits 'normal' fluorescence with a maximum near 330 nm. These facts are explained in terms of an ESIPT, which could be described in several ways:

- M1. 'Local' proton transfer with the formation of zwitterionic forms.<sup>[7–10]</sup>
- M2. Keto–enol tautomerisation (hydrogen atom transfer).<sup>[1–4]</sup>
- M3. H-chelate ring reorganisation followed by an elongation of the hydroxyl O—H bond and a decrease in the distance between the hydroxyl proton and the carboxyl oxygen.<sup>[5,11,12]</sup>

The third explanation is a variant of mechanism M2 and is mainly supported by quantum chemistry calculations.<sup>[11,12]</sup> The energy level scheme relevant to the photophysics of rotamer A is presented in Figure 1b. Population of the first singlet excited state ( $S_1$ ) is followed by a fast conversion (through proton transfer,

tautomerisation or H-chelate ring reorganisation) to the proton-transferred ( $S'_1$ ) state, which exhibits long-wave fluorescence. Besides radiative decay, the latter state is known to undergo non-radiative deactivation and intersystem crossing to the triplet state.<sup>[2]</sup> Unfortunately, information about the characteristic time scale of the  $S_1 \rightarrow S'_1$  conversion of SADs is highly scarce, but an ultrafast  $S_1 \rightarrow S'_1$  transition taking place on the femtosecond time scale can be presumed.<sup>[3,16–18]</sup>

It worth noting that most of the works devoted to SADs photophysics were carried out in non-polar and aprotic polar solvents. The excited-state dynamics of these SADs in aqueous solutions, where different forms (cationic, anionic, neutral) can exist, has been much less studied. In our recent works, the photophysics and photochemistry of salicylic and 5-sulphosalicylic acids was investigated in aqueous solutions by flash photolysis, steady state and time-resolved fluorescence.<sup>[19–21]</sup> The pH was found to be a crucial parameter that determines the photochemical and photophysical properties of these compounds.

We report here on our investigation of the photophysics of a number of SADs (salicylic, 5-sulphosalicylic, 2-methoxybenzoic and 5-aminosalicylic acids) using both the time-correlated single photon counting and the fluorescence up-conversion techniques.

\* Correspondence to: I. P. Pozdnyakov, ul. Institutskaja 3, ICK&C SB RAS, 630090 Novosibirsk, Russia.  
E-mail: pozdnyakov@ns.kinetics.nsc.ru

a I. P. Pozdnyakov, V. F. Plyusnin  
Institute of Chemical Kinetics and Combustion, Novosibirsk State University, Institutskaya 3, 630090 Novosibirsk, Pirogova 2, Russia

b A. Pigliucci, E. Vauthey  
University of Geneva, Ernest Ansermet 30, 1211 Geneva, Switzerland

c N. Tkachenko, H. Lemmetyinen  
Tampere University of Technology, 33101 Korkeakoulunkatu 8, Tampere, Finland

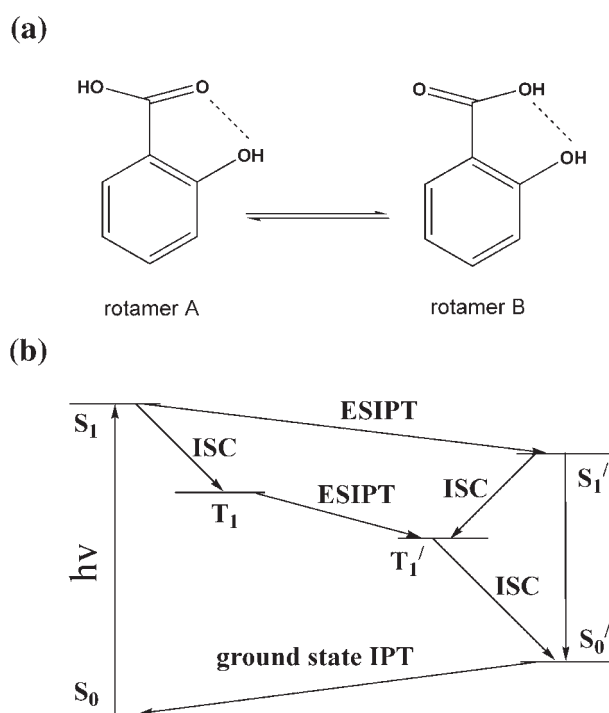


**Figure 1.** (a) Structures of the salicylic acid rotamers A and B and (b) energy level scheme pertaining to the photophysics of rotamer A

Our efforts were mainly focused on the establishment of the aforesaid mechanism of  $S_1'$  state population.

## EXPERIMENTAL

The fluorescence up-conversion setup has already been described in detail elsewhere.<sup>[22]</sup> In brief, the third harmonic of a Kerr-lens mode-locked Ti/Sapphire laser (Tsunami, Spectra-Physics) was used for excitation at 266 nm. The output pulses centred at 800 nm had duration of about 100 fs and a repetition rate of 82 MHz. The pump intensity on the samples was around  $10^{13}$  photons  $\cdot$  cm $^{-2}$   $\cdot$  pulse $^{-1}$ . The polarisation of the pump pulses was at a magic angle relative to that of the gate pulses. The full width at half maximum of the instrument response function was around 300 fs. The samples were located in a 0.4 mm thick rotating cell. The absorbance of the samples at 266 nm was 0.1–0.3. The data were analysed using the convolution of the instrument response function with the sum of two exponential functions ( $I(t, \lambda) = \sum A_i(\lambda) \exp(-t/\tau_i)$ ).

Nanosecond fluorescence dynamics was measured using the time-correlated single photon counting (TCSPC) setup described elsewhere.<sup>[23]</sup> Excitation was performed using a diode laser PLC-340 (LDH series, PicoQuant GmbH) at 350 nm and 40 MHz. The collected data were analysed analogously to the up-conversion data. The overall time resolution was 300 ps. To obtain time-resolved fluorescence spectra, all the amplitudes  $A_i(\lambda)$  were corrected for the spectral sensitivity of the PMT.

The steady-state fluorescence spectra were measured in a 1 cm cell with a 'Fluorolog' (Instruments S.A.) spectrofluorimeter. The

fluorescence quantum yields were determined by integrating the corrected emission spectra and using a solution of quinine bisulphate in 1 M H<sub>2</sub>SO<sub>4</sub> ( $\phi = 0.546$ ) as standard.<sup>[24]</sup> The absorption spectra were recorded using an Agilent 8453 spectrophotometer. All measurements were carried out at room temperature.

Sodium salicylate (Na<sub>2</sub>SA,  $\geq 99.5\%$ , Fluka), 5-sulphosalicylic (99%, Aldrich), 2-methoxybenzoic (HMBA, 99%, Aldrich) and 5-aminosalicylic (H<sub>2</sub>ASA,  $>98\%$ , Aldrich) acids were used without further purification. The solutions were prepared using bi-distilled or deionised water. The pH of the samples was adjusted by adding the required quantities of concentrated KOH or HClO<sub>4</sub> solutions (analytical grade).

## RESULTS AND DISCUSSION

### Absorption and fluorescence spectra

The absorption and emission spectra of the various forms of the SADs in aqueous solutions are depicted in Figure 2 and the main spectral parameters are summarised in Table 1. All forms of SADs exhibit a long-wave absorption band with a maximum near 300 nm ( $\pi$ - $\pi^*$  transition<sup>[11]</sup>) and a moderately high absorption coefficient ( $2$ – $3.6$ )  $\times 10^3$  M $^{-1}$   $\cdot$  cm $^{-1}$ ). Compared to the neutral forms, the ionic forms exhibit an hypsochromic shift of both the

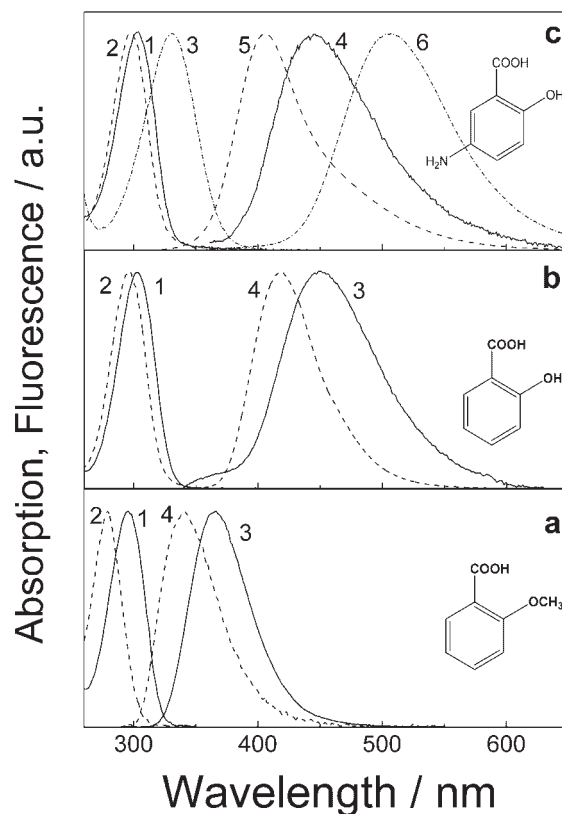


**Figure 2.** (a) Absorption (1, 2) and fluorescence (3, 4) spectra of HMBA in aqueous solutions. (1, 3) HMBA; (2, 4) MBA $^-$ . (b) absorption (1, 2) and fluorescence (3, 4) spectra of H<sub>2</sub>SA in aqueous solutions. (1, 3) H<sub>2</sub>SA; (2, 4) HSA $^-$ , (3, 6) SA $^{2-}$ . (c) absorption (1, 2, 3) and fluorescence (4, 5, 6) spectra of H<sub>2</sub>ASA in aqueous solutions. (1, 4) H<sub>3</sub>ASA $^+$ , (2, 5) H<sub>2</sub>ASA; (3, 6) HASA $^-$

**Table 1.** Spectroscopic properties of SADs. (H<sub>2</sub>SA, HSA<sup>-</sup>, SA<sup>2-</sup>—neutral form, mono- and dianion of salicylic acid; H<sub>2</sub>SSA<sup>-</sup>, HSSA<sup>2-</sup>, SSA<sup>3-</sup>—mono-, di- and trianion of 5-sulphosalicylic acid; HMBA and MBA<sup>-</sup>—neutral form and monoanion of 2-methoxybenzoic acid; H<sub>3</sub>ASA<sup>+</sup>, H<sub>2</sub>ASA and HASA<sup>-</sup>—monocation, neutral form and monoanion of 5-aminosalicylic acid)

Form	$\lambda_{\text{abs}}$ (nm)	$\epsilon$ (M <sup>-1</sup> · cm <sup>-1</sup> )	$\lambda_{\text{em}}$ (nm)	Stokes shift (cm <sup>-1</sup> )
H <sub>2</sub> SA	303	3570	450	10 800
HSA <sup>-</sup>	296	3510	408	9300
SA <sup>2-</sup>	316	3390	400	6600
H <sub>2</sub> SSA <sup>-</sup>	302	2850	440	10 400
HSSA <sup>2-</sup>	298	2770	403	8700
SSA <sup>3-</sup>	303	3360	395	7700
HMBA	296	2950	365	6400
MBA <sup>-</sup>	280	2060	340	6300
H <sub>3</sub> ASA <sup>+</sup>	303	3400	465	11 500
H <sub>2</sub> ASA	298	3340	405	8900
HASA <sup>-</sup>	332	3330	505	10 300

absorption and fluorescence bands, which is connected with a better solvation of the ionic forms in aqueous solutions

Both the neutral and ionic forms of SADs exhibit a large (>6 × 10<sup>3</sup> cm<sup>-1</sup>) Stokes shift of the fluorescence band. This suggests that the geometry of the emissive excited state differs significantly from that of the ground state, in agreement with previous photophysical investigations on the neutral forms of SADs in non-polar solvents.<sup>[1,24,5,8,9]</sup> It is worth noting that the excitation spectra of the individual forms coincide very well with their absorption spectra. The smallest Stokes shift (6300 cm<sup>-1</sup>) is found with 2-methoxybenzoic acid, where the OH group is replaced by an OCH<sub>3</sub> group. However, this shift is still too large to be considered as 'normal'.

In both the gas phase and aprotic solvents, SA are known for their tendency to form dimers, where two SA units are linked by two hydrogen bonds.<sup>[1,25]</sup> This species exhibits a new fluorescence band with a maximum at 370 nm.<sup>[1]</sup> However, no evidence of the formation dimeric SAD species was found in aqueous solutions, at least in the range of 10<sup>-5</sup>–10<sup>-2</sup> M concentration. This absence of dimerisation could be due to two different reasons:

1. The presence of the charges (for the ionic species) that leads to a Coulombic repulsion of the SADs.
2. The preferential formation of solute–solvent hydrogen bonds in aqueous media. In hydrogen-bonding solvents, the dimer is known to dissociate and SA exists in the hydrogen-bonded form.<sup>[26]</sup>

The acid–base dissociation constants of SADs in the ground (pK<sub>a</sub>) and excited (pK<sub>a</sub><sup>\*</sup>) states are listed in Table 2. These values were obtained by fitting expressions 1 and 2 for HMBA; and expressions 3 and 4 for H<sub>2</sub>SA (analogous expressions were used for H<sub>3</sub>SSA and H<sub>2</sub>ASA) to the pH-dependence of the absorbance at characteristic wavelengths, A( $\lambda$ ), and of the observed

**Table 2.** Equilibrium constants of the acid–base dissociation of SADs in the ground (pK<sub>a</sub>) and the excited (pK<sub>a</sub><sup>\*</sup>) state

	H <sub>2</sub> SA	H <sub>3</sub> SSA	HMBA	H <sub>2</sub> ASA
pK <sub>a</sub> (NH <sub>3</sub> <sup>+</sup> )	—	—	—	1.9
pK <sub>a</sub> (COOH)	2.97 (3.0 <sup>[27]</sup> )	2.8 (2.9 <sup>[28]</sup> )	3.93 (3.97 <sup>[29]</sup> )	5.7
pK <sub>a</sub> <sup>*</sup>	3.1 (3.1 <sup>[13]</sup> )	2.9	3.7	5.6

fluorescence quantum yields,  $\phi_{\text{obs}}$ , (Figure 3):

$$A(295\text{nm}) = \frac{A_{\text{HMBA}} + A_{\text{MBA}^-} \times 10^{(\text{pH}-\text{pK}_a)}}{1 + 10^{(\text{pH}-\text{pK}_a)}} \quad (1)$$

$$\phi_{\text{obs}} = \frac{\phi_{\text{HMBA}} \times (1 + K_{\text{SV}} \times 10^{-\text{pH}})^{-1} + \phi_{\text{MBA}^-} \times 10^{(\text{pH}-\text{pK}_a^*)}}{1 + 10^{(\text{pH}-\text{pK}_a^*)}} \quad (2)$$

$$A(237\text{nm}) = \frac{A_{\text{H}_2\text{SA}} + A_{\text{HSA}^-} \times 10^{(\text{pH}-\text{pK}_a)}}{1 + 10^{(\text{pH}-\text{pK}_a)}} \quad (3)$$

$$\phi_{\text{obs}} = \frac{\phi_{\text{H}_2\text{SA}} + \left( \frac{\phi_{\text{HSA}^-} \times 10^{(\text{pH}-\text{pK}_a^*)}}{1 + K_{\text{SV}} \times 10^{-\text{pH}}} \right)}{1 + 10^{(\text{pH}-\text{pK}_a^*)}} \quad (4)$$

where  $K_{\text{SV}}$  is the Stern–Volmer constant of the proton quenching of the excited state. In the case of HMBA, the  $K_{\text{SV}}$  value was directly determined from the fit of Eqn. (2) to the pH dependence

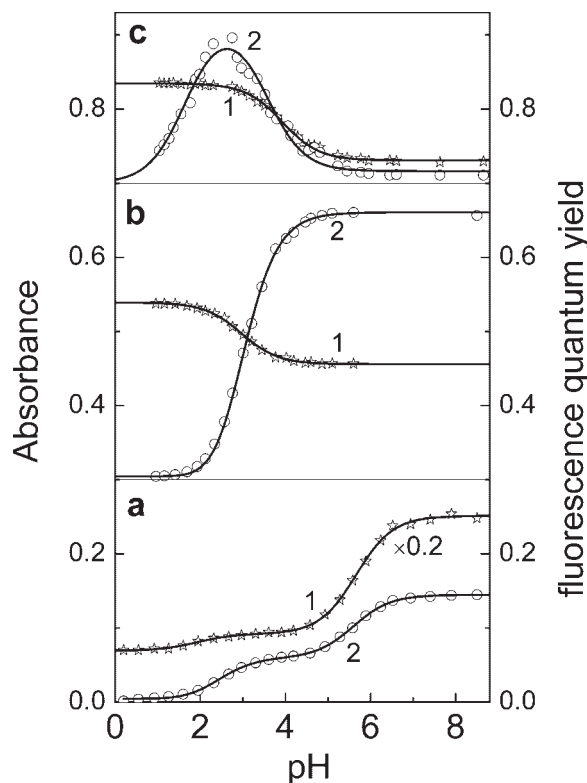


**Figure 3.** pH dependence of the absorbance at characteristic wavelengths (1) and of the observed fluorescence quantum yields (2) of H<sub>2</sub>ASA (a), H<sub>2</sub>SA (b) and HMBA (c). The smooth curves are the best fit of expressions (1–4) with the parameters listed in Tables 1 and 3

**Table 3.** Photophysical properties of the SADs in aqueous solutions

Form	$\phi_f$	$\tau_{fl}^0$ (ns)	$k_{fl} \times 10^{-7}$ (s $^{-1}$ )	$K_{SV}$ (M $^{-1}$ )	$k_q \times 10^{-10}$ (M $^{-1} \cdot$ s $^{-1}$ )
H <sub>2</sub> SA (cyclohexane)	0.02	0.46	4.3	—	—
H <sub>2</sub> SA	$\approx 4 \times 10^{-3}$	0.1	4.0	—	—
HSA $^-$	0.36	4.05 (4.2 <sup>[8]</sup> )	8.9	215	5.3
SA $^{2-}$	0.35	4.4 (4.5 <sup>[8]</sup> )	8.0	—	—
H <sub>2</sub> SSA $^-$	0.01	0.17	5.9	—	—
HSSA $^{2-}$	0.43	5.9 (6.3 <sup>[19]</sup> )	7.3	200	3.4
SSA $^{3-}$	0.18	2.3	7.8	—	—
HMBA	0.22	1.3 <sup>a</sup>	17	48	3.5
MBA $^-$	0.011	0.13 <sup>a</sup>	8.5	—	—
H <sub>2</sub> ASA(H $^+$ )	0.004	0.07	5.7	—	—
H <sub>2</sub> ASA	0.06	0.23	26	21	9.0
HASA $^-$	0.14	3.5	4.0	380	11

<sup>a</sup> Value taken from the picosecond resolved fluorescence measurements. The proton quenching of the excited state was taken into account for the calculation of  $\tau_{fl}^0$  (HMBA).

of  $\phi_{obs}$  (Table 3). For HSA $^-$ , HSSA $^{2-}$ , H<sub>2</sub>ASA and HASA $^-$ , the Stern–Volmer constants were obtained independently from nanosecond resolved fluorescence measurements (Section 3.2).

The obtained pK<sub>a</sub> values are in an excellent agreement with the known literature data (Table 2).<sup>[27–29]</sup> The acid–base dissociation constants of SADs in the excited state (pK<sub>a</sub><sup>\*</sup>) are close those of the ground state.

### Nanosecond resolved fluorescence measurements

Figure 4a presents typical fluorescence decay curves measured with salicylic acid at different pH values. In neutral solutions, the main emissive form is the monoanion HSA $^-$  that has an excited-state lifetime of  $\tau_{fl}^0 = 4.05$  ns. In strongly acid (pH < 0.5) and basic (8 M KOH) conditions, the fluorescence is predominantly due to the neutral H<sub>2</sub>SA form ( $\tau_{fl}^0 = 0.1$  ns) and to the dianion SA $^{2-}$  form ( $\tau_{fl}^0 = 4.4$  ns), respectively. At intermediate pH

values, the fluorescence kinetic exhibits a biexponential behaviour. It is worth noting that at pH < 4, the observed decrease of the HSA $^-$  fluorescence lifetime is due to the proton quenching of the excited state. Figure 4b illustrates the fit of the Stern–Volmer equation  $\frac{\tau_{fl}^0}{\tau_{fl}} = 1 + K_{SV}[H^+]$ , where  $K_{SV} = k_q \tau_{fl}^0$ , to the experimental data, that yields a quenching rate constant of HSA $^-$  of  $k_q = 3.4 \times 10^{10}$  M $^{-1} \cdot$  s $^{-1}$ . The corresponding values obtained with 5-sulphosalicylic and 5-aminosalicylic acids are presented in Table 3. The anionic forms of SADs (with the exception of MBA $^-$ ) have the largest fluorescence lifetimes, in agreement with the measured fluorescence quantum yields.

The larger  $\tau_{fl}^0$  and  $\phi_f$  values of the deprotonated SAD forms are not related to a variation of the fluorescence rate constant, the latter being practically independent of their structure and charge (Table 3). It is worth noting that in the case of salicylic and 5-sulphosalicylic acids, an analogous behaviour has been found with the triplet quantum yield and the intersystem crossing rate constant.<sup>[19,21]</sup> These observations point to a larger non-radiative decay rate constant ( $k_{NR}$ ) of the neutral and cationic forms of SADs.

The fluorescence data pertaining to the neutral form of SA in the non-polar and aprotic cyclohexane are also presented in Table 3 for comparison. In both cyclohexane and water,  $\phi_f$ ,  $\tau_{fl}^0$  and  $k_{fl}$  are of the same order of magnitude. The same was found with the triplet quantum yield and the intersystem-crossing rate constant (0.01 and 10<sup>8</sup> s $^{-1}$  in water,<sup>[20]</sup> 0.024 and 5 × 10<sup>7</sup> s $^{-1}$  in cyclohexane<sup>[2]</sup>).

### Picosecond resolved fluorescence measurements

The early fluorescence dynamics of the individual forms of SADs exhibits an initial rising component with a time constant  $\tau_1$ , additionally to the decay with time constant  $\tau_2$  also observed by TCSCP (Figure 5, Table 4). The smaller time constant  $\tau_1$  is in the range of 1–2 ps and depends weakly on the structure and charge of the SADs.

The initial rise could be assigned either to the ESIPT process, to vibrational relaxation of the ‘hot’ S<sub>1</sub> state formed by ultrafast ESIPT, or to solvent relaxation, the solvation time in water upon diffusive motion being of the order of 1 ps.<sup>[30]</sup> The first

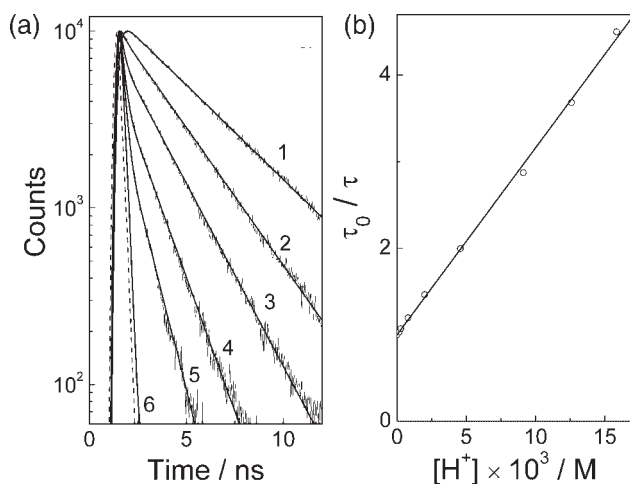


**Figure 4.** (a) Nanosecond fluorescence dynamics of salicylic acid at pH 5.7 (1), 2.7 (2), 2.3 (3), 2.0 (4), 1.8 (5) and 0.3 (6). Smooth lines: best mono- (1, 6) and two-exponential (2–5) fit after deconvolution with the instrument response function. The instrument response function is shown in dotted line. (b) Stern–Volmer plot for HSA $^-$ .

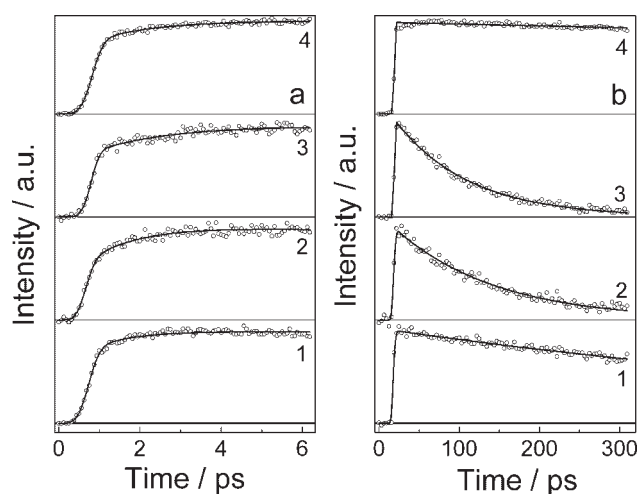


**Figure 5.** Picosecond fluorescence dynamics of HMBA (1),  $\text{MBA}^-$  (2),  $\text{H}_2\text{SA}$  (3) and  $\text{HSA}^-$  (4) on the 0–6 ps (a) and 0–300 ps (b) time scales

assumption seems to be improbable, as the characteristic ESIPT time is usually less than 200 fs.<sup>[3,16–18]</sup> Moreover, in this case, the normalised amplitude  $A_1$  should be close to unity, contrary to the experimental findings (Table 4). Solvent relaxation should not be the dominant process responsible for this rise because, in this case,  $\tau_1$  should be the same for all compounds, contrary to the observation.

As a consequence, the initial rise is most probably due to vibrational relaxation of the hot  $S'_1$  state populated upon ultrafast ESIPT. The  $\tau_1$  values (0.4–2.3 ps) are in a good agreement with known time constants of vibrational relaxation of excited molecules in solutions.<sup>[31–34]</sup> A more definite assignment of this initial rise would require measurements at several wavelengths throughout the fluorescence spectra of the SADs. This would indeed allow solvation and vibrational relaxation to be differentiated, as the first process gives rise to a red shift of the emission band, the so-called dynamic Stokes shift, while the

second one leads rather to a band narrowing.<sup>[34]</sup> However, this goes beyond the scope of the present investigation.

Unfortunately the characteristic ESIPT time cannot be deduced from the present data, most probably because of an insufficient time resolution (ca. 300 fs). Despite this, one can conclude that this process is ultrafast.

### Photophysics of SAD in aqueous solutions

After analysis of the data presented in Tables 1–4, several important statements on the photophysics of SADs in aqueous solutions can be formulated:

1. All the individual forms of the SADs exhibit a monoexponential excited-state decay and a large Stokes shift even in the case of the fully deprotonated  $\text{SA}^{2-}$  and  $\text{SSA}^{3-}$  species.
2. The fluorescence quantum yields and lifetimes of the anionic forms of SADs (with the deprotonated carboxylic group) are 10–100 times larger than those of the neutral and cationic forms due to a decrease of  $k_{\text{NR}}$ . This data is in agreement with previous results on the photophysics of SA in aqueous solutions.<sup>[8]</sup>
3. The acid–base dissociation constants of SADs in the excited state are close to those in ground state.
4. The photophysics of the neutral form of SA is similar in non-polar aprotic (cyclohexane) and polar protic (water) solvents.
5. The characteristic ESIPT time is much less than 300 fs and the time constants of vibrational cooling of the excited states of SADs are in the range of 0.4–2.3 ps.
6. The photophysical properties of 2-methoxybenzoic acid differ from those of the other compounds: the fluorescence quantum yield and lifetime of the anionic form are one order of magnitude smaller than those of the neutral form.
7. Introduction of  $\text{SO}_3\text{H}$  and  $\text{NH}_2$  groups in the 5-position on the benzene ring doesn't greatly affect the photophysical properties of SA. An analogous result has been reported for the 5-methyl and 5-*t*-butyl derivatives.<sup>[35,36]</sup>

We can now try to distinguish between the ESIPT mechanisms mentioned in the Introduction and to determine the nature of the proton-transferred state. A 'local' proton transfer with the formation of the zwitterionic excited state has to be ruled out as this mechanism contradicts statements 1 and 4. Indeed, no proton transfer should be observed with the fully deprotonated  $\text{SA}^{2-}$  and  $\text{SSA}^{3-}$  species. Similarly, the formation of the zwitterionic form in non-polar solvents is highly improbable. It worth noting that *ab initio* calculations also predict that the polar (zwitterionic) structures are not formed during ESIPT.<sup>[11,37]</sup>

Both local proton transfer and keto–enol tautomerisation mechanisms cannot explain the large Stokes shift of HMBA, which does not contain any 'transferred' proton. Moreover, the assumption of the formation of the tautomeric keto forms of SADs upon excitation does also not account for the smaller  $k_{\text{NR}}$  values of the anionic forms.

On the other hand, essentially all the experimental findings can be well explained by the model of H-chelate ring reorganisation in the excited state.<sup>[11,12]</sup> First, a single emitting species corresponding to the reorganised state is expected. Second, the elongation of the OH bond and the decrease of the distance between the OH proton and the carboxyl group oxygen should stabilise the excited state of SADs due to the enhancement of the

**Table 4.** Normalised amplitudes,  $A_i$ , and time constants,  $\tau_i$ , obtained from the biexponential fit to the fluorescence time profiles of SADs in aqueous solution

Form	$\lambda_{\text{probe}}$ (nm)	pH	$A_1$	$\tau_1^a$ (ps)	$A_2$	$\tau_2$ (ns)
$\text{H}_2\text{SA}$	420	0.8	−0.33	2.3	1.0	0.09
$\text{HSA}^-$	420	10.1	−0.23	1.5	1.0	4.05 <sup>b</sup>
$\text{SA}^{2-}$	420	8 M KOH	−0.17	1.2	1.0	4.4 <sup>b</sup>
$\text{H}_2\text{SSA}^-$	420	0.8	−0.33	1.0	1.0	0.2
$\text{HSSA}^{2-}$	420	9.5	−0.15	0.7	1.0	5.9 <sup>b</sup>
$\text{SSA}^{3-}$	420	13	−0.14	1.2	1.0	2.3 <sup>b</sup>
HMBA	380	1.9	−0.35	0.6	1.0	0.8
$\text{MBA}^-$	380	11.0	−0.41	1.1	1.0	0.13
$\text{H}_2\text{ASA}(\text{H}^+)$	420	0.5	−0.36	1.1	1.0	0.07
$\text{H}_2\text{ASA}$	420	4.2	−0.14	1.0	1.0	0.25
$\text{HASA}^-$	500	7	−0.17	0.4	1.0	3.5 <sup>b</sup>

<sup>a</sup> Error 30–50%.

<sup>b</sup> Fixed parameter.



COO<sup>-</sup>...HO hydrogen bond. Correspondingly, a decrease in  $k_{NR}$  and, as a consequence, larger fluorescence lifetimes and quantum yields have to be observed. The polarity of the reorganised state probably does not differ too much from that of the ground state, explaining why comparable photophysics were observed in both non-polar and polar solvents. Furthermore, the H-chelate ring reorganisation does not involve any great changes in the positions of the nuclei and thus this process can be expected to be ultrafast.

Finally, the photophysics of 2-methoxybenzoic acid could be explained if we assume that this compound undergoes the same excited-state processes as the other SADs. In contrast to SA, HMBA has no intramolecular hydrogen bond and therefore elongation of the O—CH<sub>3</sub> bond leads to a destabilisation of the excited state of MBA<sup>-</sup> due to a larger repulsive interaction between the COO<sup>-</sup> and CH<sub>3</sub> groups. In the case of the neutral form, the interaction between carboxylic and hydroxyl group should be much weaker explaining the observed differences in photophysical properties between the neutral and ionic forms of 2-methoxybenzoic acid (Table 3).

## CONCLUSIONS

The photophysics of several salicylic acid derivatives (SADs) in aqueous solutions was investigated in a wide range of pH using time-resolved fluorescence spectroscopy. Evidences of ESIPT were obtained for the ionic and neutral forms of salicylic, 5-aminosalicylic and 5-sulphosalicylic acids. The experimental data suggest that the photophysics of SADs in aqueous solutions should be discussed in terms of H-chelate ring reorganisation rather than hydrogen atom (proton) transfer. A deeper insight into SADs photophysics demands for an improvement of the time resolution of the fluorescence up-conversion measurements up to a few tens of femtoseconds and for quantum chemistry calculations.

## Acknowledgements

The work was supported by RFBR (06-03-32110, 06-03-90890-Mol, 05-03-39007GFEN, 07-02-91016-Fin) and the Program of complex integration projects of SB RAS-2006 (grants nos. 4.16 and 77).

## REFERENCES

- [1] P. B. Bisht, M. Okamoto, S. Hirayama, *J. Phys. Chem. B* **1997**, *101*, 8850.
- [2] H.-C. Ludemann, F. Hillenkamp, R. W. Redmond, *J. Phys. Chem. A* **2000**, *104*, 3884.
- [3] J. L. Herek, S. Pedersen, L. Banares, A. H. Zewail, *J. Chem. Phys.* **1992**, *97*, 9046.
- [4] K.-Y. Law, J. Shoham, *J. Phys. Chem.* **1995**, *99*, 12103.
- [5] L. A. Helmbrook, J. E. Kenny, B. E. Kohler, G. W. Scott, *J. Phys. Chem.* **1983**, *87*, 280.
- [6] G. S. Denisov, N. S. Golubev, Sh.S. Schreiber, V. M. Shajakhmedov, A. V. Shurukhina, *J. Mol. Struct.* **1997**, *436–437*, 153.
- [7] P. J. Kovi, C. L. Miller, S. G. Schulman, *Anal. Chim. Acta* **1972**, *61*, 7.
- [8] H. C. Joshi, H. Mishra, H. B. Tripathi, *J. Photochem. Photobiol. A: Chem.* **1997**, *105*, 15.
- [9] K. K. Smith, K. J. Kaufmann, *J. Phys. Chem.* **1978**, *82*, 2286.
- [10] A. Weller, *Z. Electrochem.* **1956**, *60*, 1144.
- [11] A. L. Sobolewski, W. Domcke, *Chem. Phys.* **1998**, *232*, 257.
- [12] E. A. El-Hakam, A. El-Nasr, A. Fujii, T. Ebata, N. Mikami, *Chem. Phys. Lett.* **2003**, *376*, 788.
- [13] A. Douhal, F. Lahmani, A. H. Zewail, *Chem. Phys.* **1996**, *207*, 477.
- [14] F. J. Stevenson, *Humus Chemistry* (2nd edn). J. Wiley & Sons, New York, **1994**.
- [15] C. Chen, S.-F. Shyu, *J. Mol. Struct. (Theochem.)* **2001**, *536*, 25.
- [16] F. V. R. Neuwahl, P. Foggi, R. G. Brown, *Chem. Phys. Lett.* **2000**, *319*, 157.
- [17] N. P. Ernsting, S. A. Kovalenko, T. Senyushkina, J. Saam, V. Farztdinov, *J. Phys. Chem. A* **2001**, *105*, 3443.
- [18] S. Ameer-Beg, S. M. Ormson, R. G. Brown, P. Matousek, M. Towrie, E. T. J. Nibbering, P. Foggi, F. V. R. Neuwahl, *J. Phys. Chem. A* **2001**, *105*, 3709.
- [19] I. P. Pozdnyakov, V. F. Plyusnin, V. P. Grivin, D. Vorobyev Yu, A. I. Kruppa, H. Lemmetyinen, *J. Photochem. Photobiol., A: Chem.* **2004**, *162*, 153.
- [20] Yu. A. Pozdnyakov, I. P. Sosedova, V. F. Plyusnin, V. P. Grivin, N. M. Bazhin, *Russ. Chem. Bull., Int. Ed.* **2007**, *56*, 1318.
- [21] I. P. Pozdnyakov, V. F. Plyusnin, V. P. Grivin, D. Vorobyev Yu, N. M. Bazhin, E. Vauthey, *J. Photochem. Photobiol., A: Chem.* **2006**, *181*, 37.
- [22] A. Morandera, L. Engeli, E. Vauthey, *J. Phys. Chem. A* **2002**, *106*, 4833.
- [23] V. Vehmanen, N. V. Tkachenko, H. Imahori, S. Fukuzumi, H. Lemmetyinen, *Spectrochim. Acta A* **2001**, *57*, 2227.
- [24] D. F. Eaton, *Pure Appl. Chem.* **1988**, *60*, 1107.
- [25] P. B. Bisht, H. Petek, K. Yoshihara, U. Nagashima, *J. Chem. Phys.* **1995**, *103*, 5290.
- [26] P. B. Bisht, H. B. Tripathi, D. D. Pant, *J. Photochem. Photobiol., A: Chem.* **1995**, *90*, 103.
- [27] L. G. Sillen, A. E. Martell, *Stability constants of metal-ion complexes*, The Chemical Society, Burlington House, **1964**.
- [28] L. S. Erre, G. Micera, F. Cariati, *Polyhedron* **1987**, *6*, 1869.
- [29] L. Varella, *Bull. Soc. Chim. France* **1955**, *22*, 872.
- [30] R. Jimenez, G. R. Fleming, P. V. Kumar, M. Maroncelli, *Nature* **1994**, *369*, 471.
- [31] P. J. Reid, C. Silva, P. F. Barbara, L. Karki, J. T. Hupp, *J. Phys. Chem.* **1995**, *99*, 2609.
- [32] S. Mitra, N. Tamai, S. Mukherjee, *J. Photochem. Photobiol. A: Chem.* **2006**, *178*, 76.
- [33] M. Sanz, A. Douhal, *Chem. Phys. Lett.* **2005**, *401*, 435.
- [34] A. Pigliucci, G. Duvanel, M. L. Lawson Daku, E. Vauthey, *J. Phys. Chem. A* **2007**, *111*, 6135.
- [35] K.-Y. Law, J. Shoham, *J. Phys. Chem.* **1995**, *99*, 12103.
- [36] F. Lahmani, A. Zehnacker-Rentien, *J. Phys. Chem.* **1997**, *101*, 6141.
- [37] S. Maheshwari, A. Chowdhury, N. Sathyamurthy, H. Mishra, H. B. Tripathi, M. Panda, J. Chandrasekhar, *J. Phys. Chem.* **1999**, *103*, 6257.